

Constraints on Cosmic Rays acceleration of Bright Gamma-ray Bursts with Observations of Fermi-LAT

Xing-Fu Zhang,^{a,b,*} Ruo-Yu Liu,^{a,b} Hai-Ming Zhang,^{a,b} Yi-Yun Huang,^{a,b} Bing Theodore Zhang^c and Xiang-Yu Wang^{a,b}

^a*School of Astronomy and Space Science, Nanjing University,
Nanjing 210023, People's Republic of China*

^b*Key Laboratory of Modern Astronomy and Astrophysics (Nanjing University), Ministry of Education,
Nanjing 210023, People's Republic of China*

^c*Center for Gravitational Physics, Yukawa Institute for Theoretical Physics,
Kyoto 606-8502, Japan*

E-mail: zhangxf@smail.nju.edu.cn

Gamma-ray bursts (GRBs) are widely suggested as potential sources of ultrahigh-energy cosmic rays (UHECRs). The kinetic energy of the jets dissipates, leading to the acceleration of protons or nuclei which interact with the intense radiation field of GRBs via the photomeson and Bethe-Heitler processes. These processes initiate a series of electromagnetic cascades, giving rise to a broadband emission up to GeV-TeV gamma-ray regime. The expected gamma-ray flux from cascades depends on properties of the GRB jet, such as the dissipation radius, the bulk Lorentz factor, and the baryon loading factor. Therefore, observations of Fermi-LAT can impose constraints on these important parameters. In this work, we calculate the cascade emissions from some bright GRBs, compare the expected fluxes with the measurements of Fermi-LAT on these GRBs, and obtain allowable ranges of aforementioned parameters. We find that the brighter the GRB is, the more stringent constraint for the baryon loading factor is obtained. For the brightest GRBs, such as GRB 221009A and 130427A, the baryon loading factor can be limited to be smaller than unity for a large ranges of dissipation radius and bulk Lorentz factor, which are much more stringent than the stacking limits based on GRB neutrino measurements. The obtained constraints from gamma rays disfavor GRBs as the main sources of UHECRs if the constraints can be generalized to all GRBs. Our results also shed some lights on the jet composition and the jet-launching mechanism.

38th International Cosmic Ray Conference (ICRC2023)
26 July - 3 August, 2023
Nagoya, Japan



*Speaker

1. INTRODUCTION

Ultrahigh-energy cosmic rays (UHECRs) are defined as those with energies exceeding $\sim 10^{18}$ eV; however, their origin remains an unresolved question [1]. The Hillas criterion suggests that the product of magnetic field strength (B) and size (R) of potential candidates must be sufficiently large [2, 3]. Gamma-ray bursts (GRBs) are the most extreme events in the universe, and their explosions lead to strong dissipation events such as shocks and magnetic reconnections that may serve as potential acceleration zones for UHECRs [3]. The magnetic field strength at these shocks is estimated to be on the order of $B \sim 10^4$ G at a distance of $R \sim 10^{14}$ cm from the center, resulting the maximum proton energies in the observer frame up to 250 EeV in typical parameters, i.e., $E_{p,\max} \simeq 250 \text{ EeV} (\frac{B}{10^4 \text{ G}}) (\frac{\Gamma_{\text{bulk}}}{400})^{-1} (\frac{R_{\text{diss}}}{10^{14} \text{ cm}}) \xi$, where Γ_{bulk} is the bulk Lorentz factor and ξ is the acceleration efficiency. Furthermore, the energy production rate density generated by GRBs can be estimated by $Q_{\text{UHECR}}^{\text{GRB}} = f_{\text{bol}} \eta_p \bar{\rho}_0 \bar{E}_{\text{iso},\gamma} = 10^{44} (\frac{\eta_p}{10}) (\frac{f_{\text{bol}}}{0.1}) (\frac{\bar{\rho}_0}{1 \text{ Gpc}^{-3} \text{ yr}^{-1}}) (\frac{\bar{E}_{\text{iso},\gamma}}{1 \times 10^{53} \text{ erg}}) \text{ erg Mpc}^{-3} \text{ yr}^{-1}$, where η_p is the baryon loading factor, f_{bol} is the fraction of accelerated protons above 10^{19} eV, $\bar{E}_{\text{iso},\gamma}$ is the average isotropic γ -ray energy budget and $\bar{\rho}_0$ is the average observed GRB rate [4]. Based on the observation of GRBs, the value of $\bar{\rho}_0$ is approximately $1 \text{ Gpc}^{-3} \text{ yr}^{-1}$ [5] and the value of $\bar{E}_{\text{iso},\gamma}$ is approximately $1 \times 10^{53} \text{ erg}$ [6]. Besides, the energy production rate density for the UHECRs at $E \sim 10^{19} - 10^{20}$ is $10^{44} \text{ erg Mpc}^{-3} \text{ yr}^{-1}$ [1], and f_{bol} is approximately 0.1 for the typical proton spectrum ($dN/dE_p \propto E_p^{-s_p}$, $s_p = 2$) [7], therefore, if UHECRs can be explained by GRBs, the product of η_p and f_{bol} should be greater than unity.

If protons (or nuclei) are accelerated to UHE in a GRB, they will interact with the intense radiations of the GRB via the photomeson and Bethe-Heitler processes, resulting in the production of neutrinos, photons, and electrons/positrons. Consequently, the information carried by these particles can be utilized to constrain UHECRs accelerated in the GRB [8–10]. For instance, based on five years data of GRBs, IceCube collaboration [11] found that for a typical bulk Lorentz factor $\Gamma_{\text{bulk}} \sim 300$, values for η_p should be less than 3, 2, and 80 in relation to the internal shock model (ISM), photospheric fireball model, and internal collision-induced magnetic reconnection and turbulence (ICMART) model respectively.

Another constraint arises from Fermi-LAT observations of individual GRBs. The interaction between the generated photons and electron pairs triggers the electromagnetic (EM) cascade, resulting in a broadband emission spanning from keV to GeV regime [12–14]. Recently, Liu et al. [15] demonstrated that the constraint derived from the GeV observation is more stringent than those obtained from the neutrino measurement for GRB 221009A, which is the brightest GRB ever recorded. Thus, the GeV observation offer an independent constraint on the GRB model, particularly for those with high keV–MeV fluxes. Therefore, we aim to generalize this method to other bright GRBs in order to investigate whether GRB 221009A represents a unique case.

2. Samples and Models

Total nine bright GRBs are selected, including GRB 221009A, GRB 130427A, GRB 180720B, GRB 190114C, GRB 160625B, GRB 190530A, GRB 160821A, GRB 160509A and GRB 131231A. There are many sources in this work, so this articles take GRB 221009A as the example.

Figure 1 shows the results of the Fermi analyses (left panel) and the timescales for various processes (right panel). It is obvious that the radiant cooling timescales (t_{syn} or t_{IC}) are much shorter than dynamic timescale (t_{dyn}), so the electron spectrum can reach quasi-steady state. We consider the Band function as the target soft photon field and typical parameters of GRBs as the benchmark, which is summarized in Table 1.

To analyze the energy distributions of secondary particles generated by photomeson and BH processes, we adopt the precise method proposed by Kelner et al.[16]. The resulting EM cascade spectrum is depicted in the left panel of Figure 2. The cascade emission is flat up to GeV and the strong magnetic field will lead to a more complicated spectrum because of the synchrotron radiation of pions (illustrated by the green dashed curve) and muons (represented by the grey dashed curve). Additionally, the cascade flux within the energy range of 0.1 to 10 GeV exhibits an approximately linear relationship with η_p , enabling us to determine the upper limit of the baryon loading factor, denoted as, η_p^{UL} , by ensuring that the flux in each bin does not exceed either the overshoot flux or the 95% confidence level upper limit of LAT. Furthermore, due to the instrumental pile-up effects, the data of $[T_0+225 \text{ s}, T_0+236 \text{ s}]$ and $[T_0+257 \text{ s}, T_0+266 \text{ s}]$ are dropped [15, 17], then the η_p^{UL} is derived from the time-interval $[T_0+200 \text{ s}, T_0+225 \text{ s}]$.

3. Results

We scan a series of radius and bulk Lorentz factor and obtain the map of η_p^{UL} , which is shown in the right panel of Figure 2. For the benchmark parameters, the value of η_p^{UL} is 0.06, which is much smaller than 10, the constraint from stacking analysis for the prompt phase[9]. Furthermore, we perform exclusion on the parameter region, such as transparent of 1 GeV photon (represented by the grey solid curve) in scenario of photospheric fireball model and the maximum radius (illustrated by the grey dashed curve) in scenario of ISM. Therefore, the allowable region is $321 \leq \Gamma_{\text{bulk}} \leq 1000$ and $4.39 \times 10^{14} \leq R_{\text{diss}} \leq 4.27 \times 10^{15} \text{ cm}$. We select some special cases and summarize corresponding results in this Table 2. η_p^{UL} are still small for case A and case B. It implies some interesting possibilities. For instance, the GRB jet may be probably dominated by leptons and magnetic field. If an efficient baryon loading factor presents in the GRB, namely $\eta_p \sim 10$, it would require larger R_{diss} and Γ_{bulk} , i.e., case C, which would support ICMART model.

One possible approach to relax the constraint on η_p^{UL} is by considering a lower acceleration efficiency, i.e., $\xi = 1\%$ or generating a softer proton spectrum, for instance, $s_p = 2.5$. We repeat the constraint and present the summarized outcome in Table 3. It shows that both $\xi = 1\%$ or $s_p = 2.5$ can relax the constraint on η_p^{UL} , however, the fraction, f_{bol} , decreases rapidly at the same time, leading to even smaller energy production rate density of UHECRs.

We apply the same methods to other GRBs and summarize the results in Table 4 and Figure 3. The values of η_p^{UL} remain small in a large parameter region, especially for GRB 130427A, which disfavors the prompt emission phase of GRBs as the main sources of UHECRs if these constraints can be generalized to all GRBs.

4. Conclusion

In summary, if protons (or nuclei) undergo acceleration in the jet, their interactions with the dense photons with energies of keV–MeV range through the photomeson process and BH process are inevitable. These interactions will result in the production of high-energy neutrinos and trigger electromagnetic cascades that ultimately generate an additional radiation component extending into the GeV–TeV range. The properties of the GRB jet, such as the dissipation radius, bulk Lorentz factor, and baryon loading factor, play a crucial role in determining the expected gamma-ray flux from cascades. Consequently, constraints on these significant parameters can be inferred through observations conducted by Fermi-LAT. In this work, we select some of the brightest GRBs from the catalog and calculate their cascade emissions.

Taking GRB 221009A as an example, the cascade emission is flat up to GeV and the strong magnetic field will lead to a more complicated spectrum because of the synchrotron radiation of pions and muons. Besides, we compared the expected cascade emission with measurements obtained by Fermi-LAT to obtain the constraints on CR acceleration in GRBs. The baryon loading factor can be limited to be smaller than 10, the constraint from stacking analysis for the prompt phase, in different cases. It implies the GRB jet may be probably dominated by leptons and magnetic field and furthermore, if considering an efficient baryon loading factor, it would require larger the dissipation radius and bulk Lorentz factor, but it would support ICMART model. Even though considering a lower acceleration efficiency and generating a softer proton spectrum can relax the constraint on the baryon loading factor, the fraction decreases rapidly at the same time, leading to even smaller energy production rate density of UHECRs. We employ identical method on all selected GRBs and find that the constraint on baryon loading factor remains stringent within a wide range of parameters, particularly in the case of GRB 130427A. These findings suggest that the prompt emission phase of GRBs is unlikely to be the primary origin of UHECRs, provided these constraint can be generalized to all GRBs. Our results also shed some lights on the jet composition and the jet-launching mechanism.

References

- [1] Valerio Verzi, Dmitri Ivanov, and Yoshiki Tsunesada. Measurement of energy spectrum of ultra-high energy cosmic rays. *Progress of Theoretical and Experimental Physics*, 2017(12):12A103, 2017.
- [2] Anthony M Hillas. The origin of ultra-high-energy cosmic rays. *Annual review of astronomy and astrophysics*, 22(1):425–444, 1984.
- [3] Kumiko Kotera and Angela V Olinto. The astrophysics of ultrahigh-energy cosmic rays. *Annual Review of Astronomy and Astrophysics*, 49:119–153, 2011.
- [4] Kohta Murase and Masataka Fukugita. Energetics of high-energy cosmic radiations. *Physical Review D*, 99(6):063012, 2019.

- [5] Enwei Liang, Bing Zhang, Francisco Virgili, and ZG Dai. Low-luminosity gamma-ray bursts as a unique population: luminosity function, local rate, and beaming factor. *The Astrophysical Journal*, 662(2):1111, 2007.
- [6] Nahliel Wygoda, Dafne Guetta, Marc-Adrien Mandich, and Eli Waxman. The energy budget of grbs based on a large sample of prompt and afterglow observations. *The Astrophysical Journal*, 824(2):127, 2016.
- [7] Shigeo S Kimura. Neutrinos from gamma-ray bursts. *arXiv preprint arXiv:2202.06480*, 2022.
- [8] Shunke Ai and He Gao. Model constraints based on the icecube neutrino nondetection of grb 221009a. *The Astrophysical Journal*, 944(2):115, 2023.
- [9] Francesco Lucarelli, Gor Oganessian, Teresa Montaruli, Marica Branchesi, Alessio Mei, Samuele Ronchini, Francesco Brighenti, Biswajit Banerjee, and Georgios Gerasimos Voutsinas. Neutrino search from γ -ray bursts during the prompt and x-ray afterglow phases using 10 years of icecube public data. *Astronomy & Astrophysics*, 672:A102, 2023.
- [10] Kohta Murase, Mainak Mukhopadhyay, Ali Kheirandish, Shigeo S Kimura, and Ke Fang. Neutrinos from the brightest gamma-ray burst? *The Astrophysical Journal Letters*, 941(1):L10, 2022.
- [11] MG Aartsen, M Ackermann, J Adams, JA Aguilar, M Ahlers, M Ahrens, I Al Samarai, D Altmann, K Andeen, T Anderson, et al. Extending the search for muon neutrinos coincident with gamma-ray bursts in icecube data. *The Astrophysical Journal*, 843(2):112, 2017.
- [12] Kai Wang, Ruo-Yu Liu, Zi-Gao Dai, and Katsuaki Asano. Hadronic origin of prompt high-energy emission of gamma-ray bursts revisited: in the case of a limited maximum proton energy. *The Astrophysical Journal*, 857(1):24, 2018.
- [13] Kohta Murase, Katsuaki Asano, Toshio Terasawa, and Peter Meszaros. The role of stochastic acceleration in the prompt emission of gamma-ray bursts: application to hadronic injection. *The Astrophysical Journal*, 746(2):164, 2012.
- [14] Katsuaki Asano, Susumu Inoue, and Peter Mészáros. Prompt x-ray and optical excess emission due to hadronic cascades in gamma-ray bursts. *The Astrophysical Journal Letters*, 725(2):L121, 2010.
- [15] Ruo-Yu Liu, Hai-Ming Zhang, and Xiang-Yu Wang. Constraints on gamma-ray burst models from grb 221009a: Gev gamma rays versus high-energy neutrinos. *The Astrophysical Journal Letters*, 943(1):L2, 2023.
- [16] SR Kelner and FA Aharonian. Energy spectra of gamma rays, electrons, and neutrinos produced at interactions of relativistic protons with low energy radiation. *Physical Review D*, 78(3):034013, 2008.
- [17] N Omodei, P Bruel, J Bregeon, M Pesce-Rollins, D Horan, E Bissaldi, R Pillera, Fermi-LAT Team, et al. Grb 221009a: Fermi lat data rate effects due to extremely high flux. *GRB Coordinates Network*, 32760:1, 2022.

Table 1: (Preliminary) The benchmark parameters in this work.

Descriptions	Parameters	Values
Bulk Lorentz Factor	Γ_{bulk}	400
Dissipation radius	R_{diss}	10^{14} cm
The index of proton injection spectrum	s_p	2
Acceleration efficiency	ξ	10%
The equipartition factors for electrons	ϵ_e	1
The equipartition factors for magnetic field	ϵ_B	1

Table 2: (Preliminary) The constraint from different cases. Case A is the constrain under the condition of the minimum Lorentz factor, $\Gamma_{\text{bulk,min}}$. Case B is the minimum η_p^{UL} in the allowable regions. Case C is the maximum η_p^{UL} in the allowable regions.

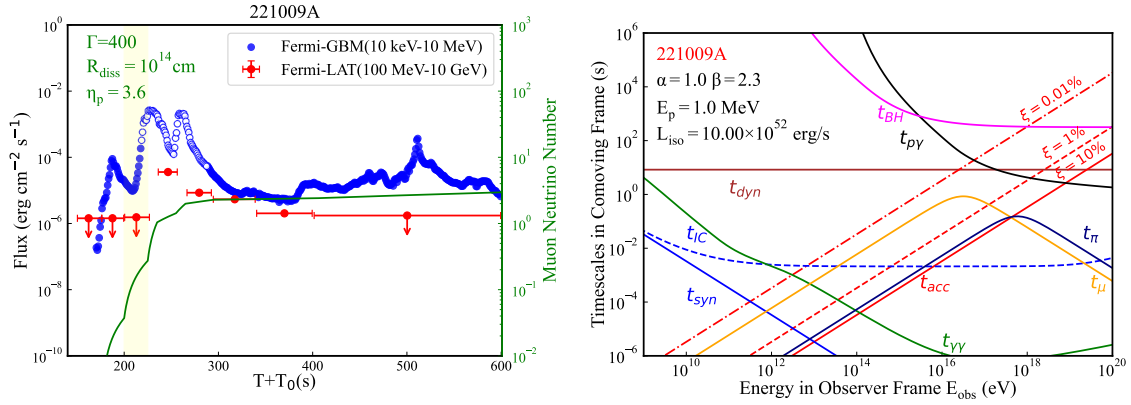
Cases	Parameters	Result
Benchmark	$(\Gamma_{\text{bulk}}, R_{\text{diss}}, \eta_p^{UL})$	(400, 1.0×10^{14} cm, 0.06)
Case A	$(\Gamma_{\text{bulk,min}}, R_{\text{diss}}, \eta_p^{UL})$	(321, 4.39×10^{14} cm, 0.08)
Case B	$(\Gamma_{\text{bulk}}, R_{\text{diss}}, \eta_{p,\text{min}}^{UL})$	(800, 1.0×10^{13} cm, 0.04)
Case C	$(\Gamma_{\text{bulk}}, R_{\text{diss,max}}, \eta_{p,\text{max}}^{UL})$	(1000, 4.27×10^{15} cm, 13.14)

Table 3: (Preliminary) The values of η_p^{UL} , f_{bol} and $Q_{\text{UHECR}}^{\text{GRB}}$ in different cases for GRB 221009A. $E_{p,\text{max}}^{\text{obs}}$ is the maximum energy of protons in observer frame.

Cases	Change	$E_{p,\text{max}}^{\text{obs}}$ (EeV)	η_p^{UL}	f_{bol}	$Q_{\text{UHECR}}^{\text{GRB}}$ (erg Mpc $^{-3}$ yr $^{-1}$)
Benchmark	-	6.06	0.06	4.0×10^{-3}	3.7×10^{40}
	$\xi = 1\%$	0.86	0.07	2.8×10^{-8}	3.1×10^{35}
	$s_p = 2.5$	6.06	3.89	5.2×10^{-6}	3.2×10^{39}
Case A	-	12.7	0.08	1.6×10^{-2}	2.0×10^{41}
	$\xi = 1\%$	1.53	0.1	1.3×10^{-5}	2.0×10^{38}
	$s_p = 2.5$	10.0	6.07	9.7×10^{-6}	9.2×10^{39}
Case B	-	2.39	0.04	1.5×10^{-4}	9.4×10^{38}
	$\xi = 1\%$	0.39	0.06	2.4×10^{-16}	2.3×10^{27}
	$s_p = 2.5$	1.22	1.27	9.8×10^{-10}	1.9×10^{35}
Case C	-	9.95	13.14	1.2×10^{-2}	2.5×10^{43}
	$\xi = 1\%$	1.0	39.54	1.9×10^{-7}	1.2×10^{39}
	$s_p = 2.5$	9.95	1991	2.2×10^{-5}	6.8×10^{42}

Table 4: (Preliminary) The properties and the results of Fermi analyses for selected GRBs. The values of η_p^{UL} are derived from the benchmark parameters.

Name	z	T_{90} (s)	F_{GBM} (erg/cm ² /s)	L_{iso} (erg/s)	F_{LAT} (erg/cm ² /s)	Ratio (= F_{GBM}/F_{LAT})	η_p^{UL}
221009A	0.151	600	1.50×10^{-3}	1.00×10^{53}	1.5×10^{-6}	1000	0.06
130427A	0.34	138	4.57×10^{-4}	1.92×10^{53}	4.75×10^{-7}	961.7	0.09
180720B	0.653	49	1.59×10^{-5}	3.18×10^{52}	4.4×10^{-8}	361.3	0.40
190114C	0.42	116	5.66×10^{-5}	3.91×10^{52}	6.23×10^{-7}	90.8	1.02
160625B	1.406	35.1	4.63×10^{-5}	6.13×10^{53}	1.81×10^{-7}	255.8	4.51
190530A	0.936	18.4	3.33×10^{-5}	1.61×10^{53}	2.95×10^{-7}	112.9	1.70
160821A	0.4	43	4.66×10^{-5}	2.87×10^{52}	5.58×10^{-8}	835	0.17
160509A	1.17	369.7	1.94×10^{-5}	1.63×10^{53}	2.47×10^{-7}	78.5	3.91
131231A	0.642	31.2	3.98×10^{-6}	7.61×10^{51}	5.9×10^{-8}	67.2	3.44

**Figure 1:** (Preliminary) Left panel: 0.1–10 GeV light curve observed by Fermi-LAT (red circles or ULs) in comparison with the 10 keV–10 MeV light curve observed by Fermi-GBM (blue circles) for GRB 221009A. The yellow shadows are the time intervals chosen for calculating the upper limit for η_p . The open blue circles in GRB 221009A represent the data which are under the influence of the pile-up effects. The green curve represents the expected cumulative $\bar{\nu}_\mu + \nu_\mu$ event number in IceCube in the case of $\Gamma = 400$, $R_{diss} = 10^{14}$ cm, which is normalized by adjusting η_p . Right panel: timescales in the comoving frame of various processes. The black and pink solid curves represent the energy loss timescales of protons via the $p\gamma$ and BH processes respectively. The blue solid and dashed curves show the cooling timescales of electrons via the synchrotron and IC radiation respectively. The green curve shows the timescale of the fifth generation $\gamma\gamma$ absorption. The solid brown curve present the dynamical timescale of the energy dissipation. The navy and orange solid curves are the cooling timescales of pion and muon, respectively. The red solid, dashed and dotted-dashed curves represent the acceleration timescales for $\xi = 10\%$, $\xi = 1\%$ and $\xi = 0.01\%$, respectively. We plot all panels in the benchmark case. The parameters of Band function and corresponding luminosity are shown in the upper left corners.

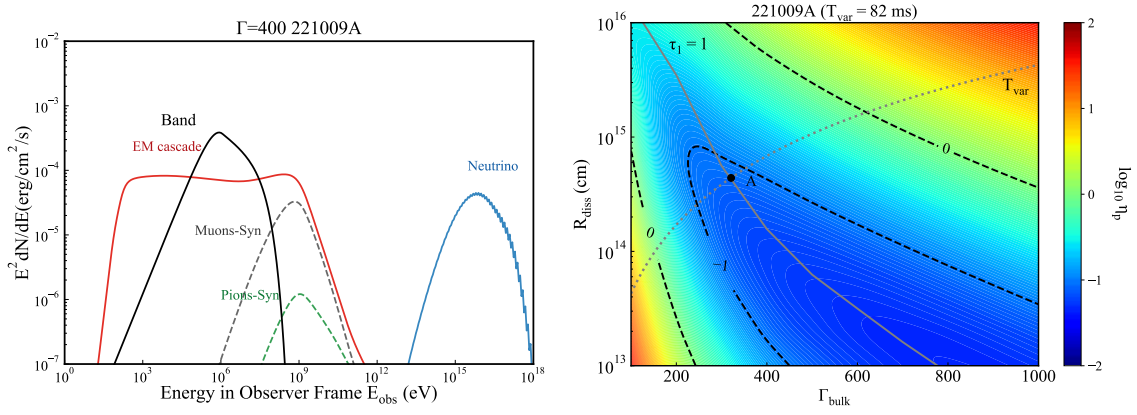


Figure 2: (Preliminary) Left panel: Predicted spectral energy distributions (SEDs) of the EM cascade emission (red curves) and the high-energy neutrino emission (blue curves) in benchmark parameters. The black curves represent the SED of the Band component. Individual contributions of muons synchrotron and pions synchrotron are denoted by grey dashed curves and green dashed curves as labeled, respectively. The SEDs of the EM cascade emission has considered the self-synchrotron absorption and $\gamma\gamma$ absorption. Right panel: The baryon loading factor in logarithmic form ($\log_{10}\eta_p$) map as a function of R_{diss} and Γ_{bulk} for GRB 221009A. The gray dotted lines represent the maximum dissipation radius in the scenario of ISM. The gray solid lines depict the R_{diss} and Γ_{bulk} corresponding to 1 GeV photon with the opacity of unity ($\tau_1 = 1$). The black dots (A) denote the points of intersection between the two curves, which correspond to the minimum Γ_{bulk} .

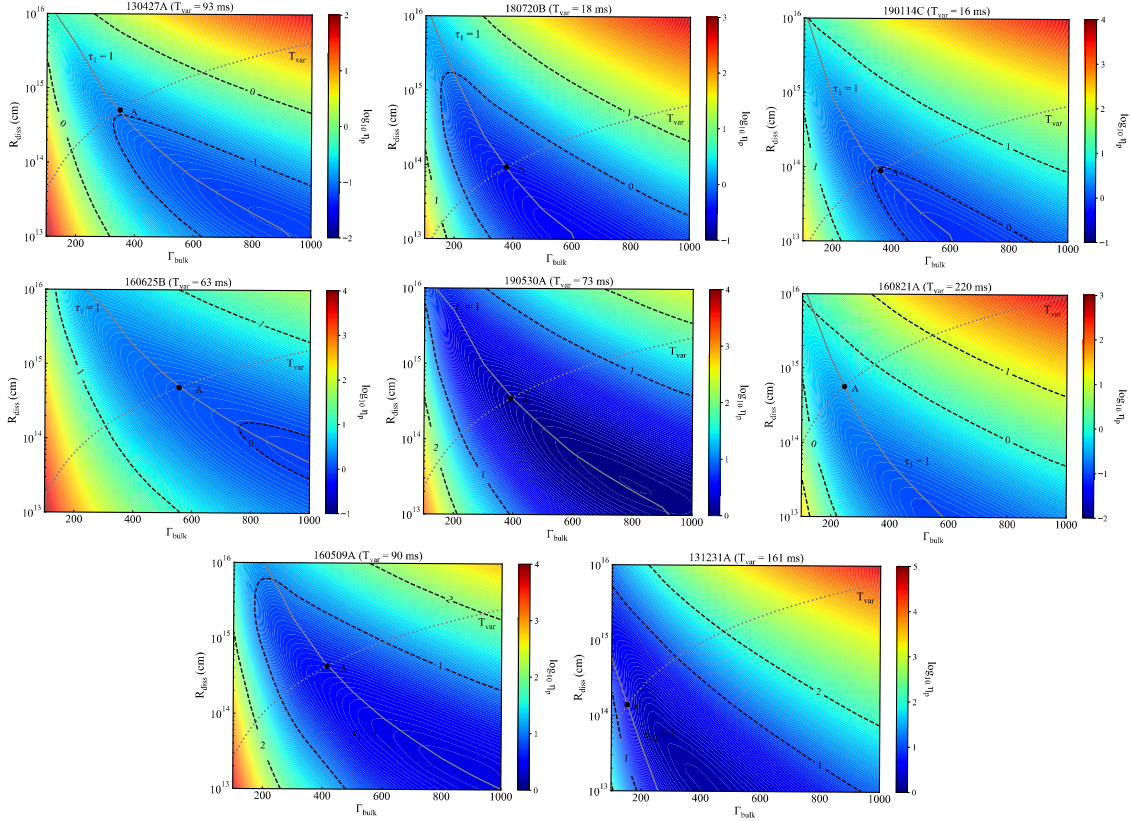


Figure 3: (Preliminary) Same as the right panel of Figure 2, but for selected GRBs.